An *in vivo* correlate of exercise-induced neurogenesis in the adult dentate gyrus

Ana C. Pereira*†, Dan E. Huddleston*†, Adam M. Brickman*†, Alexander A. Sosunov‡, Rene Hen§, Guy M. McKhann‡, Richard Sloan§, Fred H. Gage¶, Truman R. Brown‖, and Scott A. Small*†**

*The Taub Institute for Research on Alzheimer's Disease and the Aging Brain, Departments of †Neurology, ‡Neurosurgery, §Psychiatry, and ‖Radiology, Columbia University College of Physicians and Surgeons, New York, NY 10032; and ¶The Salk Institute, La Jolla, CA 92037

Contributed by Fred H. Gage, December 30, 2006 (sent for review November 26, 2006)

With continued debate over the functional significance of adult neurogenesis, identifying an *in vivo* correlate of neurogenesis has become an important goal. Here we rely on the coupling between neurogenesis and angiogenesis and test whether MRI measurements of cerebral blood volume (CBV) provide an imaging correlate of neurogenesis. First, we used an MRI approach to generate CBV maps over time in the hippocampal formation of exercising mice. Among all hippocampal subregions, exercise was found to have a primary effect on dentate gyrus CBV, the only subregion that supports adult neurogenesis. Moreover, exercise-induced increases in dentate gyrus CBV were found to correlate with postmortem measurements of neurogenesis. Second, using similar MRI technologies, we generated CBV maps over time in the hippocampal formation of exercising humans. As in mice, exercise was found to have a primary effect on dentate gyrus CBV, and the CBV changes were found to selectively correlate with cardiopulmonary and cognitive function. Taken together, these findings show that dentate gyrus CBV provides an imaging correlate of exercise-induced neurogenesis and that exercise differentially targets the dentate gyrus, a hippocampal subregion important for memory and implicated in cognitive aging.

hippocampus | *in vivo* imaging | cerebral blood volume | angiogenesis

The hippocampal formation, a brain circuit made up of separate but interconnected subregions (1), is vital for memory function (2) and is targeted by the aging process (3). The dentate gyrus is the only hippocampal subregion that supports neurogenesis in the adult brain (4–6). Nevertheless, because neurogenesis can only be assessed in postmortem tissue, its functional significance remains undetermined. With this limitation in mind, we have explored different imaging approaches applicable to rodents and humans that might provide an *in vivo* correlate of neurogenesis.

Although imaging radioligands designed to bind newly dividing cells is an attractive approach, positron emission tomography imaging suffers inherently poor resolution and cannot visualize the dentate gyrus. Additionally, radiolabeling newborn cells introduces potential safety concerns. For these reasons, we have focused on MRI technologies instead. Notably, a coupling has been established between neurogenesis and angiogenesis (7, 8). The process of angiogenesis, in turn, gradually gives rise to the formation of new blood vessels, increasing regional microvascular density (9–12). Importantly, vascular density can be measured *in vivo* with imaging techniques that map regional blood volume. Numerous studies have established a tight relationship between angiogenesis and regional blood volume (13–17), including in the brain where regional angiogenesis is coupled to regional cerebral blood volume (CBV) (18–26).

Because CBV can be measured with MRI, we hypothesized that a regionally selective increase in hippocampal CBV might provide an imaging correlate of neurogenesis. This hypothesis was tested in mice in which *in vivo* imaging and postmortem analysis can be performed on the same subjects. We used an MRI approach that can generate hippocampal CBV maps repeatedly and safely over time in mice while simultaneously assessing multiple hippocampal subregions (27). We exploited the capabilities of this approach to establish how hippocampal CBV maps change during physical exercise, a potent stimulant of dentate gyrus neurogenesis (28), and tested whether CBV changes correlate with postmortem measurements of neurogenesis. Once these findings were established in mice, we were interested in determining how exercise affects the hippocampal CBV maps of humans. To accomplish this goal, we first optimized an MRI approach (29) previously shown to be capable of generating hippocampal CBV maps in non-human primates (30) and then charted exercise-induced CBV changes in the human hippocampal formation.

Results

Exercise Selectively Increases Dentate Gyrus CBV in Mice and Correlates with Neurogenesis. In designing our experimental protocol, we were guided by the observation that angiogenesis-induced sprouting of new blood vessels progresses through different stages, forming gradually over time (9). Accordingly, mice were allowed to exercise for 2 weeks, the period during which neurogenesis reaches its maximum increase, and bromodeoxyuridine (BrdU), a marker of newly born cells, was injected daily during the second week. To capture the predicted delayed effect in CBV, mice were kept alive for 4 more weeks, then killed and processed for BrdU labeling. Hippocampal CBV maps (Fig. 1*b*) assessing the entorhinal cortex, the dentate gyrus, and the CA3 and CA1 subfields were generated four times over the 6-week experiment: at preexercise baseline and at weeks 2, 4, and 6. A control group following the identical protocol but without exercise was imaged in parallel.

A repeated-measure ANOVA was used to analyze the imaging data set (Fig. 1*a*). A group–time interaction was found only for the dentate gyrus, showing that exercise was associated with a selective increase in dentate gyrus CBV ($F = 5.0$, $P = 0.034$). As shown by simple contrasts, the effect was driven by a maximum increase that emerged 2 weeks after the cessation of exercise, from week 2 to week 4 ($F = 5.9$, $P = 0.021$) (Fig. 1*a*). The entorhinal cortex was the only other hippocampal subregion whose CBV increased appreciably over time, although not achieving statistical significance (Fig. 1*a*). Although exercise might potentially affect CBV by increasing metabolism and cerebral blood flow, previous studies (31, 32) have shown that exercise-induced changes in metabolism should manifest during, not after, the exercise regimen. Thus, the observed spatiotemporal profile with which CBV emerged fits better with a model of exercise-induced angiogenesis in the dentate gyrus.

In agreement with previous studies (33), the exercise group was found to have greater BrdU labeling compared with the nonexercise group ($F = 9.8$, $P = 0.004$) (Fig. 2*a*). More than 90% of

Author contributions: G.M.M., R.S., F.H.G., and S.A.S. designed research; A.C.P., D.E.H., A.M.B., and A.A.S. performed research; R.H. and T.R.B. contributed new reagents/analytic tools; and A.C.P., F.H.G., and S.A.S. wrote the paper.

The authors declare no conflict of interest.

Abbreviation: CBV, cerebral blood volume.

**To whom correspondence should be addressed. E-mail: sas68@columbia.edu.

This article contains supporting information online at www.pnas.org/cgi/content/full/0611721104/DC1.

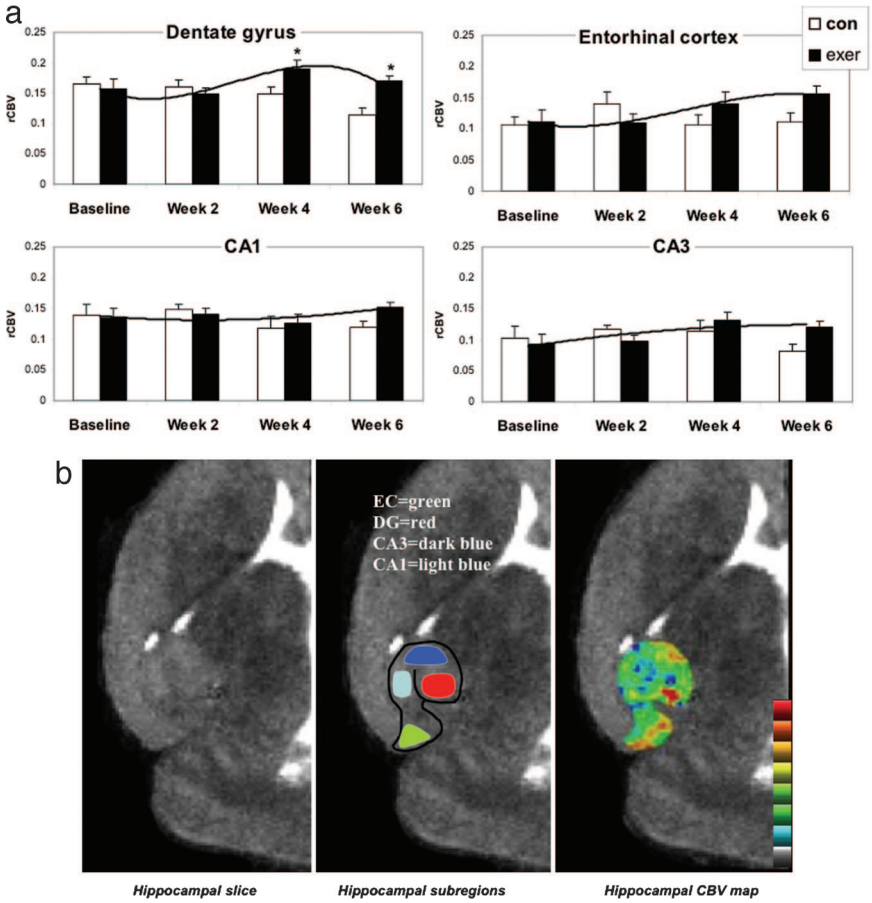

Fig. 1. Exercise selectively increases dentate gyrus CBV in mice. (*a*) Exercise had a selective effect on dentate gyrus CBV. Bar graphs show the mean relative CBV (rCBV) values for each hippocampal subregion in the exercise group (filled bars) and the nonexercise group (open bars) over the 6-week study. The dentate gyrus was the only hippocampal subregion that showed a significant exercise effect, with CBV peaking at week 4, whereas the entorhinal cortex showed a nonsignificant increase in CBV. (*b*) An individual example. (*Left*) High-resolution MRI slice that visualizes the external morphology and internal architecture of the hippocampal formation. (*Center*) Parcellation of the hippocampal subregions (green, entorhinal cortex; red, dentate gyrus; dark blue, CA3 subfield; light blue, CA1 subfield). (*Right*) Hippocampal CBV map (warmer colors reflect higher CBV).

BrdU-positive cells colabeled for NeuN, a neuron-specific marker (Fig. 2*a*). To examine the relationship between neurogenesis and CBV, the repeated-measures model was again used and included BrdU as a covariate. A significant time-by-BrdU interaction was observed only for dentate gyrus CBV ($F = 3.3$, $P = 0.039$), driven primarily by changes from week 2 to week 4 ($F = 8.8$, $P = 0.006$). As shown by a direct analysis, this effect reflected a positive correlation between BrdU and changes in CBV from week 2 to week 4 ($\beta = 0.58$, $P = 0.001$) (Fig. 2*b*). Of note, when BrdU was included as a covariate in the ANOVA, the group–time effect observed in the dentate gyrus was no longer significant, confirming that neurogenesis accounted for the exercise effect on CBV. Visual inspection of the relationship between changes in dentate gyrus CBV and BrdU (Fig. 2*b*) suggested that a quadratic vs. a linear model better characterized the relationship, which was confirmed by curve estimation analysis (linear model, $R^2 = 0.34$ and $P = 0.001$; quadratic model, $R^2 = 0.59$ and $P < 0.0001$). Thus, the association between changes in dentate gyrus CBV and BrdU exists primarily when CBV increases with exercise (Fig. 2*b*). Finally, to test whether neurogenesis was required for the observed increases in dentate gyrus CBV we relied on a previously described x-irradiation approach that selectively blocks dentate gyrus neurogenesis (55). Four mice received x-irradiation, and three mice were sham controls. After a 3-month recovery period, all mice were imaged by using the exercise protocol. A repeated-measure ANOVA applied to the CBV data set revealed a group (x-ray vs. sham)-by-time interaction only for the dentate gyrus ($F = 7.6$, $P = 0.04$), showing that irradiation blocked the exercise-induced increases in CBV [supporting information (SI) Fig. 5].

Exercise Selectively Increases Dentate Gyrus CBV in Humans and Correlates with Aerobic Fitness and Cognition. Once we established that dentate gyrus CBV provides a correlate of exercise-induced neurogenesis, we were interested in testing whether this effect is observed in exercising humans. CBV maps of the human hippocampal formation were generated by using our previously reported MRI approach, specifically tailored for imaging the primate hippocampal formation (30). Eleven healthy subjects (mean age = 33, ranging from 21–45 years; two males and nine females) participated in the study, completing a 3-month aerobic exercise regimen. Hippocampal CBV maps were generated before and after exercise. CBV values were reliably measured for all hippocampal subregions, except the CA3 subregion (Fig. 3*b*). Compared with experimental animals, in humans it is impossible to control the interindividual differences in physical activity performed during daily life. Therefore, before and after exercise, we measured the maximum volume of oxygen consumption (VO_2max), the gold standard measure of exercise-associated aerobic fitness (34, 35) to quantify individual differences in degree of exercise. Cognitive performance was assessed by using a modified Rey Auditory Verbal Learning Test (36), whose design allows cognition to be tested across different learning trials and during delayed recall, recognition, and source

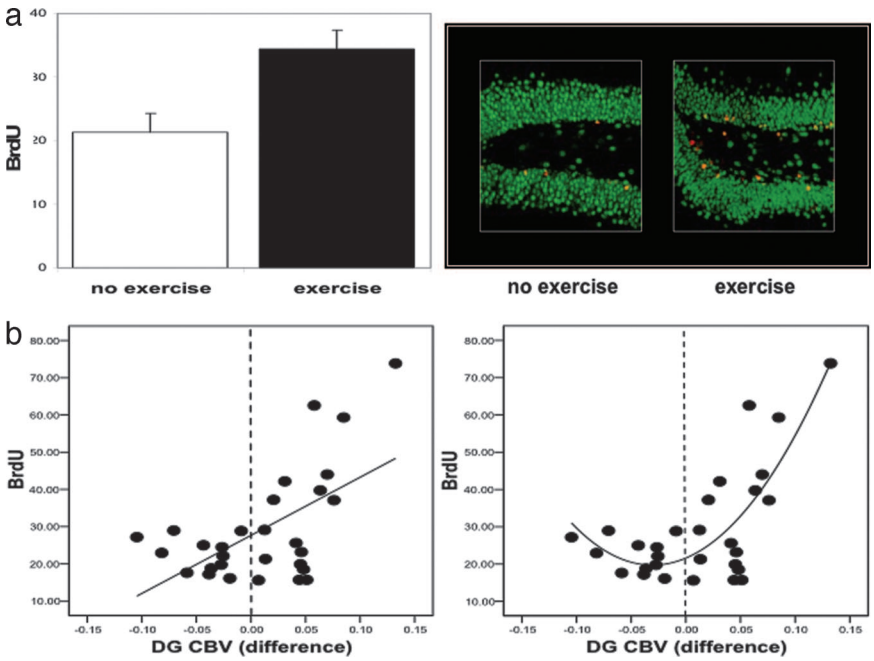

Fig. 2. Exercise-induced increases in dentate gyrus CBV correlate with neurogenesis. (*a*) (*Left*) Exercising mice were found to have more BrdU labeling compared with the no-exercise group. (*Right*) As shown by confocal microscopy, the majority of the new cells were colabeled with NeuN (red, BrdU labeling; green, NeuN; yellow, BrdU/NeuN double labeling). (*b*) (*Left*) A significant linear relationship was found between changes in dentate gyrus CBV and BrdU labeling. (*Right*) A quadratic relationship better fits the data. The vertical stippled line in each plot splits the *x* axis into CBV changes that decreased (left of line) versus those that increased (right of line) with exercise.

memory. Ten subjects were cognitively assessed after exercise, eight of whom were assessed at preexercise baseline.

A repeated-measures ANOVA used to analyze the imaging data showed that the dentate gyrus was the only hippocampal subregion whose CBV significantly increased over time ($F = 12$, $P = 0.006$) (Fig. 3*a*). As in mice, the entorhinal cortex was the only other hippocampal subregion whose CBV increased appreciably over time, although not achieving statistical significance ($F = 4.3$, $P = 0.064$) (Fig. 3*a*). As a group, VO_2max values significantly increased over time ($F = 11.6$, $P = 0.007$) (Fig. 4*a*), and, to confirm that the imaged changes were directly related to exercise and not simply caused by a test–retest effect, we found that individual differences in dentate gyrus CBV were correlated to individual changes in VO_2max ($\beta = 0.662$, $P = 0.027$) (Fig. 4*b*). Importantly, a correlation between CBV and VO_2max was not observed for any other hippocampal subregion, including the entorhinal cortex (Fig. 4*b*), confirming that exercise has a selective effect on dentate gyrus CBV.

Cognitively, individuals performed significantly better on trial 1 learning ($F = 7.0$, $P = 0.027$) after exercise, with a trend toward improvement on all-trial learning ($F = 5.0$, $P = 0.053$) and delayed recall ($F = 5.0$, $P = 0.057$). There was no effect on delayed recognition ($F = 0.19$, $P = 0.67$) or source memory ($F = 0.15$, $P = 0.25$) (Fig. 4*a*). To test that cognitive improvement was related to exercise *per se*, we found that individual changes in trial 1 learning were correlated with individual changes in VO_2max ($\beta = 0.660$, $P = 0.037$). However, because only 8 of the 10 subjects completed preexercise cognitive testing, we repeated the analysis with postexercise cognitive performance scores. Again, we found that changes in VO_2max correlated exclusively with postexercise trial 1 learning ($\beta = 0.70$, $P = 0.026$) (Fig. 4*b*). Additional analyses showed that the correlation between changes in VO_2max and cognition was selective to trial 1 learning (Fig. 4*b*), thereby confirming that, despite apparent increases in other cognitive measures (i.e., delayed recognition, as shown in Fig. 4*a*), this particular measure was selectively influenced by exercise.

Finally, we examined the relationship between cognition and CBV. Among all hippocampal subregions, the correlation between improvements in trial 1 performance and increases in dentate gyrus CBV was the only one that trended toward significance ($\beta = 0.62$, $P = 0.052$). Because of the missing preexercise data, we repeated all of the analyses comparing changes in CBV with postexercise cognition, finding an exclusive correlation between postexercise trial 1 learning and dentate gyrus CBV ($\beta = 0.63$, $P = 0.026$) (Fig. 4*b*).

Discussion

Taken together, our findings show that, within the hippocampal formation, exercise targets the dentate gyrus with regional selectivity. In addition, our results identify that, in mice, dentate gyrus CBV is an imaging correlate of exercise-induced neurogenesis.

Because of its pleiotropic effect on the brain (37, 38), the subregional selectivity that exercise was found to have within the hippocampal formation was an unexpected finding. This observation is particularly interesting in light of studies suggesting that the dentate gyrus is a hippocampal subregion differentially vulnerable to the aging process, as shown in humans (39, 40), nonhuman primates (30, 41), and rodents (30, 42), and that dentate gyrus dysfunction contributes to cognitive aging (30, 40). Interestingly, a growing number of studies have established that exercise ameliorates age-related cognitive decline (43–46). Thus, the effect that exercise was observed to have on the dentate gyrus likely contributes to the reported cognitive benefits exercise has on the aging brain.

Because neurogenesis couples with angiogenesis (7, 8) and angiogenesis, in turn, couples with CBV (18–26), we hypothesized that measures of CBV might provide an *in vivo* correlate of neurogenesis. This hypothesis is based in part on our previous findings that exercise increases both neurogenesis and angiogenesis in young adult rodents (43). We have confirmed this prediction with our high-resolution MRI techniques, which are capable of assessing individual hippocampal subregions, showing that dentate gyrus

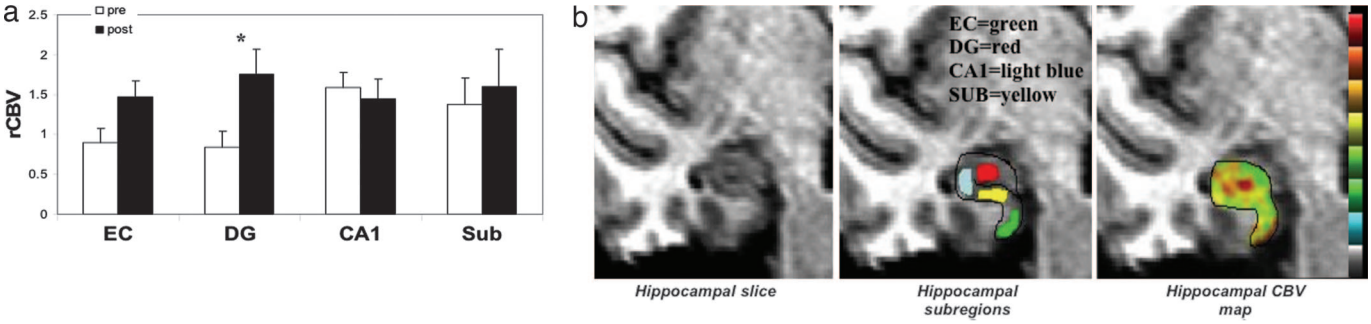

Fig. 3. Exercise selectively increases dentate gyrus CBV in humans. (*a*) Exercise had a selective effect on dentate gyrus CBV. Bar graph shows the mean relative CBV (rCBV) values for each hippocampal subregion before exercise (open bars) and after exercise (filled bars). As in mice, the dentate gyrus was the only hippocampal subregion that showed a significant exercise effect, whereas the entorhinal cortex showed a nonsignificant increase in CBV. (*b*) An individual example. (*Left*) High-resolution MRI slice that visualizes the external morphology and internal architecture of the hippocampal formation. (*Center*) Parcellation of the hippocampal subregions (green, entorhinal cortex; red, dentate gyrus; blue, CA1 subfield; yellow, subiculum). (*Right*) Hippocampal CBV map (warmer colors reflect higher CBV).

CBV selectively correlates with underlying neurogenesis in mice. Blocking the exercise-induced CBV effect with irradiation, a neurogenesis suppressant, further confirms that neurogenesis underlies the observed increases in CBV. However, in the absence of direct measurements, we have not confirmed that angiogenesis is the intermediate factor that accounts for this relationship. Mechanistically, there are many molecules that may be mediating the exercise-induced coupling between neurogenesis and angiogenesis (47), including VEGF (8) or exercise-induced changes in BDNF (48).

The remarkable similarities between the exercise-induced CBV changes in the hippocampal formation of mice and humans suggest that the effect is mediated by similar mechanisms. Of course, in contrast to mice, it is impossible to directly confirm whether the changes in dentate gyrus CBV observed in humans are a reflection of neurogenesis. Nevertheless, previous rodent studies have shown that levels of neurogenesis are coupled with individual differences in degree of exercise (28). Therefore, together with the cross-species similarities on hippocampal CBV, the observation that exercise-induced changes in dentate gyrus CBV correlate with VO_2max supports the interpretation that the human effect is mediated, at least in part, by neurogenesis.

In any case, our results show that *in vivo* imaging can predict levels of neurogenesis in living mice. Furthermore, as demonstrated, the MRI technologies used in these studies are capable of measuring meaningful changes in dentate gyrus CBV over time in both humans and mice. By providing evidence in support of exercise-induced neurogenesis and by introducing the tools needed to achieve this goal, this study shows that it is possible to isolate the specific profile of cognitive changes that are neurogenesis-dependent. Furthermore, the imaging tools presented here are uniquely suited to investigate potential pharmacological modulators of neurogenesis, testing their role in treating depression (49) and in ameliorating the cognitive decline that occurs in all of us as we age (43, 50).

Methods

Exercise. ***Mice.*** A total of 46 C57BL/6 mice (7 weeks old) were used (23 exercising and 23 nonexercising animals). The experimental mice were placed in cages with running wheels (Lafayette Instrument Company, Lafayette, IN). The animals ran voluntarily for 2 weeks. MRI images were acquired at the following time points: week 0 (baseline), week 2 (when exercise was stopped), week 4, and week 6. The thymidine analog BrdU marker was injected i.p. for 7 consecutive days (60 $mg \cdot kg^{-1} \cdot day^{-1}$) during the second week of the experiment. At week 6, the animals were anesthetized and killed in accordance with institutional guidelines.

Human. Eleven subjects (mean age, 33 ranging from 21–45 years; 2 males and 9 females) who fulfilled the American Heart Association criteria for below-average aerobic fitness (VO_2max, <43 for men and <37 for women) were recruited (51). The 11 enrolled subjects engaged in an exercise training protocol for 12 weeks at Columbia University Fitness Center at a frequency of four times a week. Each exercise session lasted ≈1 h: 5 min of low-intensity warm-up on a treadmill or stationary bicycle, 5 min of stretching, 40 min of aerobic training, and 10 min for cool down and stretching. During the 40 min of aerobic activity, subjects were permitted to select from cycling on a stationary ergometer, running on a treadmill, climbing on a StairMaster, or using an elliptical trainer.

VO_2max was measured by a graded exercise test on an Ergoline 800S electronic-braked cycle ergometer (SensorMedics, Anaheim, CA). Each subject began exercising at 30 W for 2 min, and the work rate was continually increased by 30 W each 2 min until VO_2max criteria (respiratory quotient of ≥ 1.1, increases in ventilation without concomitant increases in VO_2, maximum age-predicted heart rate, and/or volitional fatigue) were reached. Minute ventilation was measured by a pneumotachometer connected to a FLO-1 volume transducer module (Physio-Dyne Instrument Corporation, Quogue, NY). Percentages of expired oxygen (O_2) and carbon dioxide (CO_2) were measured by using a paramagnetic O_2 analyzer and an infrared CO_2 analyzer connected to a computerized system (MAX-1; Physio-Dyne Instrument Corporation). These analyzers were calibrated against known medical grade gases. The highest VO_2 value attained during the graded exercise test is considered VO_2max.

In Vivo* Imaging.** ***Mice. Mice were imaged with a 9.4-T Bruker scanner (AVANCBV 400WB spectrometer; Bruker NMR, Billerica, MA) by following a previously described protocol (27). Briefly, axial T2-weighted images were optimally acquired with a fast sequence (time to repeat/effective echo time = 2,000 ms/70 ms; 30-mm i.d. birdcage radio frequency probe; shielded gradient system, 100 g/cm; rapid acquisition with relaxation enhancement factor, 16; field of view, 19.6 mm; acquisition matrix, 256 × 256; no. of slices, 8; slice thickness, 0.6 mm; slice gap, 0.1 mm; number of excitations, 28). Five sets of images were acquired sequentially, each requiring 16 min. The first two sets were precontrast. Gadodiamide was then injected (13 mmol/kg i.p.) through a catheter placed intraperitoneally before imaging. The last three sets corresponded to the postcontrast images. To prevent head motion and reduce anxiety, the animals were anesthetized with isoflurane gas [1.5% (vol/vol) for maintenance at 1 liter per minute of air flow) via a nose cone. Isoflurane was chosen because it induces minimal cerebral hemodynamic change (52). Monitoring of the heart rate, respiratory rate, and oxygen saturation was performed during the whole

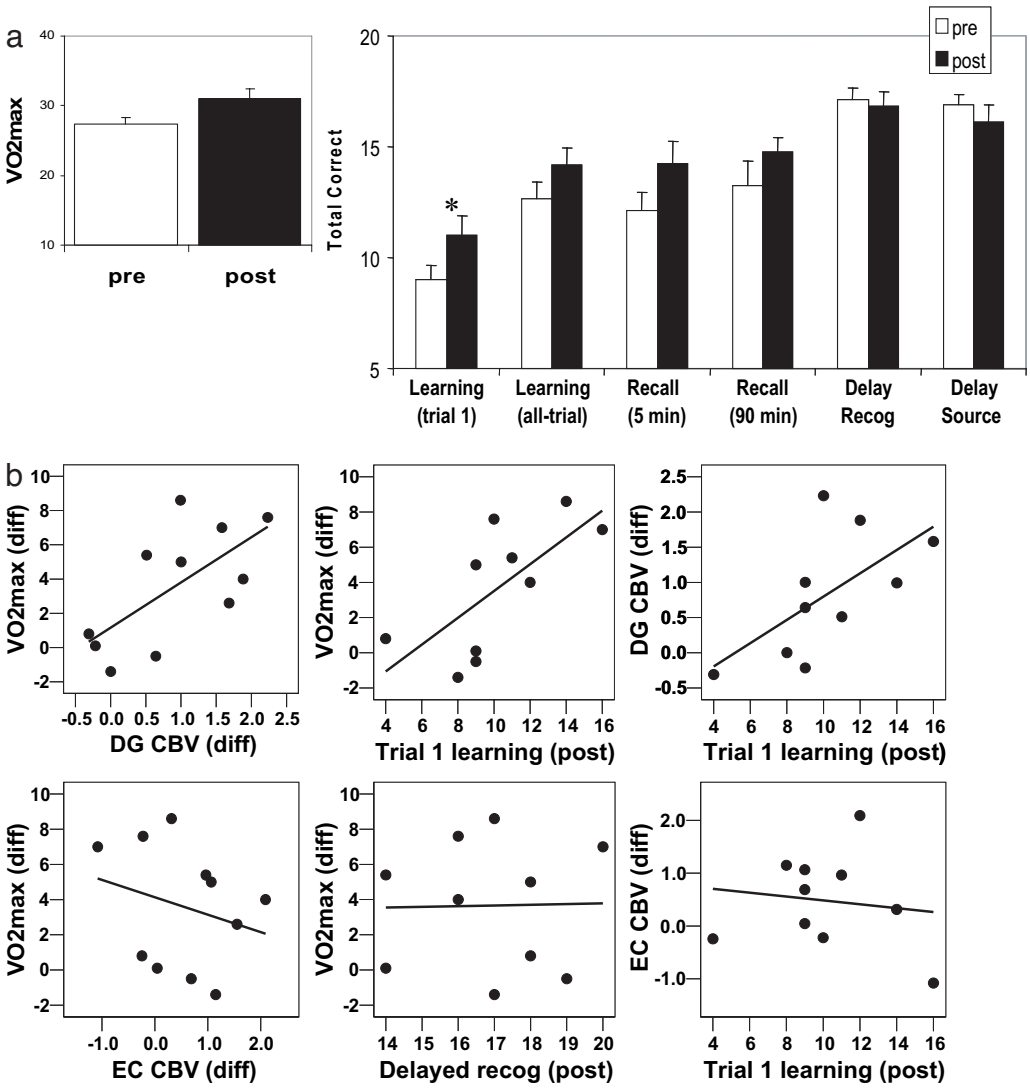

Fig. 4. Exercise-induced increases in dentate gyrus CBV correlate with aerobic fitness and cognition. (*a*) (*Left*) VO_2max, the gold-standard measure of exercise-induced aerobic fitness, increased after exercise. (*Right*) Cognitively, exercise has its most reliable effect on first-trial learning of new declarative memories. (*b*) (*Left*) Exercise-induced changes in VO_2max correlated with changes in dentate gyrus (DG) CBV but not with other hippocampal subregions, including the entorhinal cortex (EC), confirming the selectivity of the exercise-induced effect. (*Center*) Exercise-induced changes in VO_2max correlated with postexercise trial 1 learning but not with other cognitive tasks, including delayed recognition. (*Right*) Postexercise trial 1 learning correlated with exercise-induced changes in dentate gyrus CBV but not with changes in other hippocampal subregions, including the entorhinal cortex.

procedure. Relative CBV was mapped as changes of the transverse relaxation rate (ΔR^2) induced by the contrast agent. When the contrast agent reaches uniform distribution, CBV maps can be measured from steady-state T2-weighted images as CBV $\propto \Delta R^2 = \ln(S_{pre}/S_{post})/TE$, where TE is the effective echo time, S_{pre} is the signal before the contrast administration, and S_{post} is the signal after the contrast agent reaches steady-state. To control for differences in levels of contrast administration, cardiac output, and global blood flow, the derived maps were normalized to the maximum 4-pixel signal value of the posterior cerebral vein. Visualized anatomical landmarks were used together with standard atlases to identify the localization of four hippocampal subregions: the dentate gyrus, the CA3 subfield, the CA1 subfield, and the entorhinal cortex (53). The normalized CBV measurements from each subregion were used for group data analysis.

Human. Subjects were imaged with a 1.5-T scanner Intera scanner (Philips, Amsterdam, The Netherlands). As previously described (30), coronal T1-weighted images (repetition time, 20 ms; echo time, 6 ms; flip angle, 25°; in-plane resolution, 0.86 × 86 mm; slice thickness, 4 mm) were acquired oriented perpendicular to the hippocampal long-axis before and 4 min after i.v. administration of the contrast gadolinium (0.1 mmol/kg). The difference between precontrast and postcontrast images was used to access the regional CBV map. To control for differences in levels of contrast administration, cardiac output, and global blood flow, the derived differences in signal intensity were normalized to the maximum 4-pixel signal value of the sagittal sinus (29). For each subject, the precontrast scan was used to identify the slice with the best visualization of the external morphology and internal architecture of the hippocampal formation. Visualized anatomical landmarks were used together with standard atlases to identify the general locale of four subregions: the dentate gyrus, the CA1 subfield, the subiculum, and the entorhinal cortex (30). The normalized CBV measurements from each subregion were used for group data analysis.

Microscopy. ***Immunohistochemistry.*** Free-floating, 40-μm coronal sections were used in the determination of BrdU labeling. DNA denaturation was conducted by incubation for 1 h at 2 M HCl at

37°C, followed by washing in boric buffer (pH 8.5). After washing, sections were incubated for 30 min in 10% H_2O_2 to eliminate endogenous peroxidases. After blocking with 3% normal donkey serum in 0.2% Triton X-100, sections were incubated with monoclonal anti-BrdU (1:600; Roche, Basel, Switzerland) overnight at 4°C. Sections were then incubated for 1 h at room temperature with the secondary antibody (biotinylated donkey anti-mouse; Jackson ImmunoResearch Laboratories, West Grove, PA) followed by amplification with an avidin–biotin complex (Vector Laboratories, Burlingame, CA), and visualized with diaminobenzidine (Sigma, St. Louis, MO). For double-immunolabeling, free-floating sections were incubated in a mixture of primary antibodies, anti-BrdU (1:600; Roche), and anti-NeuN (1:500; Chemicon, Temecula, CA), raised in different species overnight. For visualization, Alexa Fluor-conjugated appropriate secondary antibodies (1:300; Molecular Probes, Eugene, OR) raised in goats were used for 1 h at room temperature. Blocking serum and primary and secondary antibodies were applied in 0.2% Triton X-100 in PBS. Sections for fluorescent microscopy were mounted on slides in VECTASHIELD (Vector Laboratories). For control of the specificity of immunolabeling, primary antibodies were omitted and substituted with appropriate normal serum. Slides were viewed with a confocal microscope [Radiance 2000 (Bio-Rad, Hercules, CA) mounted on a E800 microscope (Nikon, Tokyo, Japan)]. The images presented are stacks of six to 16 optical sections (step, 1 mm) that were collected individually (in the green and red channels) or simultaneously with precaution against cross-talk between channels. The images were processed with PhotoShop 7.0 (Adobe Systems, San Jose, CA) without contrast and brightness changes in split images.

Quantitation of BrdU labeling. Every sixth section throughout the hippocampus was processed for BrdU immunohistochemistry. Ten sections were used for each animal. All BrdU-labeled cells in the dentate gyrus (granule cell layer and subgranular zone) were counted under a light microscope by an experimenter blinded to the study code. The average number of BrdU-labeled cells was then derived for each animal.

Cognitive testing. Declarative memory was measured with a version of the Rey Auditory Verbal Learning Test (36) modified to increase variability in memory performance among healthy young adults. Twenty nonsemantically or phonemically related words were presented over three learning trials in which the test administrator read the word list and the subject free-recalled as many words as possible. Administration of the three learning trials was immediately followed by one learning trial of a distracter list and then a short delayed free recall of the initial list. After a 90-min delay period, subjects were asked to freely recall words from the initial list and then to freely recall items from the distracter list. After a 24-hr delay period, subjects were contacted by telephone and asked to freely recall items from the initial list and then from the distracter list. They were then administered a forced-choice recognition trial in which they were required to identify the 20 words from the initial learning trial among semantically and phonemically related words, as well as words from the distracter trial. Finally, a source memory trial was administered in which subjects were read a list containing only words from the initial learning list and from the distracter list and were asked to identify from which list each word came. Two forms of the verbal learning test were created, and the administration order was counterbalanced. As in previous studies (54), we measured words correctly recalled on the first trial of the initial learning trials, the average number of words recalled across the three learning trials, the number of words from the initial learning trial that were correctly recalled after a short delay (<5 min), the number of words from the initial learning trial that were correctly recalled after a 90-min delay, the number of items correctly identified on the recognition trial, and the correct number of items identified on the source memory trial.

We thank Kenneth Hess and Fan Hau for help in mouse imaging and Clay Lacefield for helping deliver x-irradiation. This work was supported by grants from the Defense Advanced Research Projects Agency, the National Institutes of Health (AG025161), the New York Heart Association, the Lookout Foundation, and the James S. McDonnell Foundation.

1. Amaral DG (1993) *Curr Opin Neurobiol* 3:225–229.
2. Squire LR, Stark CE, Clark RE (2004) *Annu Rev Neurosci* 27:279–306.
3. Erickson CA, Barnes CA (2003) *Exp Gerontol* 38:61–69.
4. Altman J, Das GD (1965) *J Comp Neurol* 124:319–335.
5. Kaplan MS, Hinds JW (1977) *Science* 197:1092–1094.
6. Eriksson PS, Perfilieva E, Bjork-Eriksson T, Alborn AM, Nordborg C, Peterson DA, Gage FH (1998) *Nat Med* 4:1313–1317.
7. Palmer TD, Willhoite AR, Gage FH (2000) *J Comp Neurol* 425:479–944.
8. Louissaint A, Jr, Rao S, Leventhal C, Goldman SA (2002) *Neuron* 34:945–960.
9. Carmeliet P (2003) *Nat Med* 9:653–660.
10. Risau W (1998) *Kidney Int Suppl* 67:S3–S6.
11. McDonald DM, Choyke PL (2003) *Nat Med* 9:713–725.
12. D'Amore PA, Thompson RW (1987) *Annu Rev Physiol* 49:453–464.
13. Mayr NA, Hawighorst H, Yuh WT, Essig M, Magnotta VA, Knopp MV (1999) *J Magn Reson Imaging* 10:267–276.
14. Taylor JS, Tofts PS, Port R, Evelhoch JL, Knopp M, Reddick WE, Runge VM, Mayr N (1999) *J Magn Reson Imaging* 10:903–907.
15. Bremer C, Mustafa M, Bogdanov A, Jr, Ntziachristos V, Petrovsky A, Weissleder R (2003) *Radiology* 226:214–220.
16. Kerwin W, Hooker A, Spilker M, Vicini P, Ferguson M, Hatsukami T, Yuan C (2003) *Circulation* 107:851–856.
17. van Dijke CF, Brasch RC, Roberts TP, Weidner N, Mathur A, Shames DM, Mann JS, Demsar F, Lang P, Schwickert HC (1996) *Radiology* 198:813–818.
18. Dennie J, Mandeville JB, Boxerman JL, Packard SD, Rosen BR, Weisskoff RM (1998) *Magn Reson Med* 40:793–799.
19. Cha S, Johnson G, Wadghiri YZ, Jin O, Babb J, Zagzag D, Turnbull DH (2003) *Magn Reson Med* 49:848–855.
20. Pathak AP, Rand SD, Schmainda KM (2003) *J Magn Reson Imaging* 18:397–403.
21. Dunn JF, Roche MA, Springett R, Abajian M, Merlis J, Daghlian CP, Lu SY, Makki M (2004) *Magn Reson Med* 51:55–61.
22. Lin TN, Sun SW, Cheung WM, Li F, Chang C (2002) *Stroke* 33:2985–2991.
23. Sugahara T, Korogi Y, Kochi M, Ikushima I, Hirai T, Okuda T, Shigematsu Y, Liang L, Ge Y, Ushio Y, Takahashi M (1998) *Am J Roentgenol* 171:1479–1486.
24. Maia AC, Jr, Malheiros SM, da Rocha AJ, da Silva CJ, Gabbai AA, Ferraz FA, Stavale JN (2005) *Am J Neuroradiol* 26:777–783.
25. Aronen HJ, Pardo FS, Kennedy DN, Belliveau JW, Packard SD, Hsu DW, Hochberg FH, Fischman AJ, Rosen BR (2000) *Clin Cancer Res* 6:2189–2200.
26. Jiang Q, Zhang ZG, Ding GL, Silver B, Zhang L, Meng H, Lu M, Pourabdillah-Nejed DS, Wang L, Savant-Bhonsale S, *et al.* (2006) *NeuroImage* 32:1080–1089.
27. Moreno H, Hua F, Brown T, Small S (2006) *NMR Biomed* 19:535–543.
28. van Praag H, Kempermann G, Gage FH (1999) *Nat Neurosci* 2:266–270.
29. Lin W, Celik A, Paczynski RP (1999) *J Magn Reson Imaging* 9:44–52.
30. Small SA, Chawla MK, Buonocore M, Rapp PR, Barnes CA (2004) *Proc Natl Acad Sci USA* 101:7181–7186.
31. Vissing J, Andersen M, Diemer NH (1996) *J Cereb Blood Flow Metab* 16:729–736.
32. Ide K, Secher NH (2000) *Prog Neurobiol* 61:397–414.
33. van Praag H, Christie BR, Sejnowski TJ, Gage FH (1999) *Proc Natl Acad Sci USA* 96:13427–13431.
34. Mitchell JH, Sproule BJ, Chapman CB (1958) *J Clin Invest* 37:538–547.
35. Wagner PD (1996) *Annu Rev Physiol* 58:21–50.
36. Rey A (1964) *L'Examen Clinique en Psychologie* (Presses Univ de France, Paris).
37. Cotman CW, Berchtold NC (2002) *Trends Neurosci* 25:295–301.
38. Dishman RK, Berthoud HR, Booth FW, Cotman CW, Edgerton VR, Fleshner MR, Gandevia SC, Gomez-Pinilla F, Greenwood BN, Hillman CH, *et al.* (2006) *Obesity (Silver Spring)* 14:345–356.
39. West MJ, Coleman PD, Flood DG, Troncoso JC (1994) *Lancet* 344:769–772.
40. Small SA, Tsai WY, DeLaPaz R, Mayeux R, Stern Y (2002) *Ann Neurol* 51:290–295.
41. Gazzaley AH, Siegel SJ, Kordower JH, Mufson EJ, Morrison JH (1996) *Proc Natl Acad Sci USA* 93:3121–3125.
42. Shetty AK, Turner DA (1999) *Exp Neurol* 158:491–503.
43. van Praag H, Shubert T, Zhao C, Gage FH (2005) *J Neurosci* 25:8680–8685.
44. Kramer AF, Hahn S, Cohen NJ, Banich MT, McAuley E, Harrison CR, Chason J, Vakil E, Bardell L, Boileau RA, Colcombe A (1999) *Nature* 400:418–419.
45. Chan AS, Ho YC, Cheung MC, Albert MS, Chiu HF, Lam LC (2005) *J Am Geriatr Soc* 53:1754–1760.
46. Weuve J, Kang JH, Manson JE, Breteler MM, Ware JH, Grodstein F (2004) *J Am Med Assoc* 292:1454–1461.
47. Emanueli C, Schratzberger P, Kirchmair R, Madeddu P (2003) *Br J Pharmacol* 140:614–619.
48. Neeper SA, Gomez-Pinilla F, Choi J, Cotman CW (1996) *Brain Res* 726:49–56.
49. Santarelli L, Saxe M, Gross C, Surget A, Battaglia F, Dulawa S, Weisstaub N, Lee J, Duman R, Arancio O, *et al.* (2003) *Science* 301:805–809.
50. Small SA, Stern Y, Tang M, Mayeux R (1999) *Neurology* 52:1392–1396.
51. Fletcher GF, Balady G, Froelicher VF, Hartley LH, Haskell WL, Pollock ML (1995) *Circulation* 91:580–615.
52. Lei H, Grinberg O, Nwaigwe CI, Hou HG, Williams H, Swartz HM, Dunn JF (2001) *Brain Res* 913:174–179.
53. Paxinos G, Franklin K (2001) *The Mouse Brain in Stereotaxic Coordinates* (Academic, Philadelphia).
54. Van der Elst W, van Boxtel MP, van Breukelen GJ, Jolles J (2005) *J Int Neuropsychol Soc* 11:290–302.
55. Santarelli L, Saxe M, Gross C, Surget A, Battaglia F, Dulawa S, Weisstaub N, Lee J, Duman R, Arancio O, *et al.* (2003) *Science* 301:805–809.